EOF-Based Linear Prediction Algorithm: Examples

KWANG-Y. KIM AND GERALD R. NORTH

Climate System Research Program, Department of Meteorology, Texas A&M University, College Station, Texas

(Manuscript received 5 February 1998, in final form 29 July 1998)

ABSTRACT

Considered here are examples of statistical prediction based on the algorithm developed by Kim and North. The predictor is constructed in terms of space–time EOFs of data and prediction domains. These EOFs are essentially a different representation of the covariance matrix, which is derived from past observational data. The two sets of EOFs contain information on how to extend the data domain into prediction domain (i.e., statistical prediction) with minimum error variance. The performance of the predictor is similar to that of an optimal autoregressive model since both methods are based on the minimization of prediction error variance. Four different prediction techniques—canonical correlation analysis (CCA), maximum covariance analysis (MCA), principal component regression (PCR), and principal oscillation pattern (POP)—have been compared with the present method. A comparison shows that oscillation patterns in a dataset can faithfully be extended in terms of temporal EOFs, resulting in a slightly better performance of the present method than that of the predictors based on the maximum pattern correlations (CCA, MCA, and PCR) or the POP predictor. One-dimensional applications demonstrate the usefulness of the predictor. The NINO3 and the NINO3.4 sea surface temperature time series (3-month moving average) were forecasted reasonably up to the lead time of about 6 months. The prediction skill seems to be comparable to other more elaborate statistical methods. Two-dimensional prediction examples also demonstrate the utility of the new algorithm. The spatial patterns of SST anomaly field (3-month moving average) were forecasted reasonably up to about 6 months ahead. All these examples illustrate that the prediction algorithm is useful and computationally efficient for routine prediction practices.

1. Introduction

This study examines the performance of a general statistical prediction algorithm developed in Kim and North (1998). In particular, the algorithm is applied to detecting the spatiotemporal patterns of El Niño. El Niño is the largest, short-term interannual climatic fluctuation over the tropical Pacific Ocean characterized by the occurrence of a warm water mass in the eastern Pacific. Prediction of El Niños is of great importance, since they have significant impacts on the global and local climate, environment, and economy.

El Niño is known to be a quasi-periodic disturbance of the earth's climate system with the period varying between 2 and 6 yr. Not only the periodicity but also the spatiotemporal structure of El Niño are different from one event to another, seemingly an extremely difficult phenomenon to predict. Improved prediction skill of El Niño over recent years employing dynamical models, however, indicates that El Niño is more predictable than was first thought. The extended prediction skill is usually attributed to internal ocean dynamics. The so-called delayed oscillator concept (Suarez and Schopf 1988; Graham and White 1988; Battisti and Hirst 1989; Cane et al. 1990; Münnich et al. 1991) is accepted by many.

In the context of the delayed oscillator, the onset and termination of El Niño (warm) and La Niña (cold) are treated as ''cyclic'' implying ''a priori'' predictability. Statistical methods are good for predicting such quasi-cyclic disturbances. Indeed, earlier statistical approaches have shown that El Niño is predictable at about 6-month lead time or longer. This predictability surely comes from the occurrence of low-frequency variability in the data (Barnett et al. 1988, 1994). In this study, a new statistical predictor is applied to El Niño as a demonstration of its performance and utility.

The predictor in this study is constructed based on space–time empirical orthogonal functions (EOFs) of the predictand field. These EOFs represent the eigenfunctions of the covariance matrix of a predictand field. The covariance statistics, in turn, represent our knowledge on the predictand field from past observational data. Then, a prediction filter is constructed using EOFs such that prediction error variance is minimized according to our knowledge of the predictand field. Our knowledge, of course, is incomplete both due to the insufficiency of data and the stochastic component in

Corresponding author address: Dr. Kwang-Y. Kim, Climate System Research Program, Department of Meteorology, Texas A&M University, College Station, TX 77843-3150.
E-mail: kykim@csrp.tamu.edu

the predictand field, and the predictor is only as good as our knowledge derived from the past records.

The performance of the predictor should be similar to that of an autoregressive (AR) predictor (with an optimal order) since both methods are based on the minimization of prediction error variance. The latter uses a temporal covariance matrix directly in the form of the prediction normal equations (Newton 1988) while the former uses EOFs that are derived from a covariance matrix (Kim and North 1998). Although the latter assumes the form of a one-dimensional predictor, it can be used for two-dimensional prediction in a manner similar to the present predictor. Namely, the independence of the principal component (PC) time series of EOFs allows them to be predicted individually via an AR predictor. One essential difference of the present predictor, however, is the prediction in both the space and the time domains while the AR prediction is limited only to time. Also, the EOF representation of the predictand field allows us to examine and preferentially select the EOF modes, both in space and time, that are beneficial for prediction.

One of main motivations for the EOF representation of the predictor is the simplicity and the completeness of an EOF basis set. Some methods employ principal oscillation patterns (POPs), or complex normal modes, because moving patterns of El Niño can be represented better in terms of a group of complex POPs than stationary patterns like EOFs. Then, prediction is conducted in terms of complex POP coefficients and eigenvalues that contain information on how the resolved spatial patterns (POPs) evolve in time (Xu and von Storch 1990; Penland and Magorian 1993). In the present study, a POP representation has not been considered because POP modes do not form an orthogonal basis set (Hasselmann 1988; von Storch et al. 1995). Due to the use of regular EOFs instead of POPs, the present method will be inferior to those using POPs in resolving the moving patterns of El Niño. Thus, one may have to use many EOFs instead of a few POPs (e.g., Penland and Magorian 1993). In the present technique, temporal evolution of spatial patterns is extracted from the PC time series of EOFs. Unlike POPs, which have unique decay (*e*-folding) times and oscillation periods attached to them, temporal evolution of each EOF pattern is given in terms of temporal EOFs of the corresponding PC time series. In essence, temporal EOFs show how the matching spatial pattern evolves in time. The resolution of temporal oscillation patterns in terms of temporal EOFs certainly deserves attention and works well, as will be demonstrated in the examples.

In some other studies complex EOFs or extended EOFs are used to represent the moving spatial patterns of El Niño (Graham et al. 1987a,b; Barnett et al. 1988). Again, complex EOFs or extended EOFs are better than regular EOFs in resolving moving patterns. The beauty of the present algorithm is that it can easily be implemented in terms of any set of orthogonal basis functions. Thus, complex EOFs and extended EOFs are suitable basis functions to build the predictor. In fact, the use of cyclostationary empirical orthogonal functions (CSEOFs) as a basis set for the predictor is currently being considered since El Niño is strongly phase locked to the annual cycle of the tropical sea surface temperature (SST) field and its phase and prediction depend sensitively on the time of the year.

As a cross validation and a comparison of the performance the predictor will be compared with four other predictors. They are the predictors based on the POP technique, the maximum covariance method (MCA), the canonical correlation method (CCA), and the principal component regression method (PCR). These predictors were developed in the EOF space of the predictand field.

The present technique as applied to a PC time series T_i can be written as

$$T_i(t) = \sum_{t' \in \mathcal{D}} \Gamma(t, t')T_i(t'), \qquad t \in \mathcal{R}, \tag{1}$$

where $\Gamma(t, t')$ is the prediction filter (kernel), and $\mathcal{D}$ and $\mathcal{R}$ are called the data domain and prediction domain, respectively. Future values of $T_i(t)$ are predicted by applying a filter to observed values of $T_i(t)$. A prediction filter is specifically tailored for each dataset and is constructed in terms of EOFs (e.g., Fig. 1). The prediction algorithm is described in detail in Kim and North (1998).

The POP technique essentially finds the period and the damping scale of oscillation patterns in a dataset that allow the prediction of the POP coefficient time series (Penland 1989; Xu and von Storch 1990; Penland and Magorian 1993). A POP model is given by

$$T_i(t + 1) = \sum_j A_{ij}T_j(t) + \epsilon_i(t), \tag{2}$$

where i and j are EOF mode numbers. The so-called system matrix is obtained by

$$\mathbf{A} = \mathbf{C}(1)\mathbf{C}(0)^{-1}. \tag{3}$$

Here $\mathbf{C}(n)$ is the lag-n spatial covariance matrix of $\{T_i(t)\}$. An eigen analysis of the system matrix yields eigenvalues λ_n and eigenfunctions P_n, which are called the POPs. Since the system matrix is not symmetric POPs and eigenvalues may be, in general, complex. [See the detailed introduction to the technique by J.-S. von Storch (1995).] Then, the Green's function at any arbitrary lag τ is given by (Penland 1989)

$$\mathbf{G}(\tau) = \sum_n P_n(\lambda_n)^\tau Q_n^{\mathrm{T}}, \tag{4}$$

where P_n and Q_n are, respectively, the nth POP and adjoint POP patterns, namely,

$$P_nQ_n^{\mathrm{T}} = Q_nP_n^{\mathrm{T}} = \mathbf{I}, \tag{5}$$

where the superscript T denotes transposition and $\mathbf{I}$ is an identity matrix. The POP prediction, then, is given by

$$T_i(t + \tau) = \sum_j G_{ij}(\tau)T_j(t). \quad (6)$$

The POP prediction consists essentially of finding spatial patterns and their decay and oscillation timescales in terms of complex POP eigenvalues.

The CCA analysis (Glahn 1968) finds a set of pairs of eigenvectors (P_k, Q_k) from two datasets $\{X_i(t)\}$ and $\{Y_i(t)\}$ so that (see also von Storch 1995)

$$X_i(t) = \sum_k \alpha_k(t)P_{ki} \quad \text{and} \quad Y_i(t) = \sum_k \beta_k(t)Q_{ki}, \quad (7)$$

where P_{ki} and Q_{ki} are the ith components of the eigenvectors P_k and Q_k, respectively. The PC time series $\{\alpha_k(t) | k = 1, 2, \ldots\}$ constitute a set of independent random variables and so do the PC time series $\{\beta_k(t) | k = 1, 2, \ldots\}$. That is,

$$\langle \alpha_k(t)\alpha_l(t)\rangle = \delta_{kl} \quad \text{and} \quad \langle \beta_k(t)\beta_l(t)\rangle = \delta_{kl}, \quad (8)$$

where $\langle \cdot \rangle$ represents an ensemble average and δ is the Kronecker delta. Further, the two sets are also independent of each other. Namely,

$$\langle \alpha_k(t)\beta_l(t)\rangle = 0, \quad \text{for all } k \neq l. \quad (9)$$

A pair of eigenvectors, say mode number k, is determined such that the corresponding PC time series have the maximum correlation for given $k - 1$ modes. The mode number is arranged such that the correlation of a lower mode is larger than that of a higher mode.

In prediction, the CCA technique is used to maximize the correlation between the predictand and the transformed predictor fields (Graham et al. 1987a, b; Barnett et al. 1988). In terms of the predictor field $X(t)$, predictand field $Y(t)$ is given by (Yu et al. 1997)

$$Y_i(t) = \sum_j H_{ij}X_j(t), \quad (10)$$

where the predictor matrix $\mathbf{H}$ is given by

$$\mathbf{H} = \mathbf{Q}^{-1}\mathbf{AP}. \quad (11)$$

Here $\mathbf{P} = \{P_1, P_2, \ldots\}$ and $\mathbf{Q} = \{Q_1, Q_2, \ldots\}$ and $\mathbf{A}$ is a diagonal matrix, each diagonal component of which is the square root of the eigenvalues, that is,

$$\mathbf{A} = \text{Diag}(\sqrt{\lambda_1}, \sqrt{\lambda_2}, \ldots). \quad (12)$$

The MCA analysis is similar in spirit to the CCA analysis (Bretherton et al. 1992; Wallace et al. 1992; von Storch and Zwiers 1998). Instead of trying to achieve maximum correlations between two sets of PC time series, the MCA analysis aims at finding a pair of PC time series that share maximum covariance of the datasets. It was found that the performance of a predictor based on the MCA technique is a little better than that of the CCA technique (Bretherton et al. 1992; Wallace et al. 1992).

The PCR analysis is, in essence, expressed by (Draper and Smith 1981; Yu et al. 1997)

$$Y_i(t) = \sum_j R_{ij}X_j(t) + e_i(t), \quad (13)$$

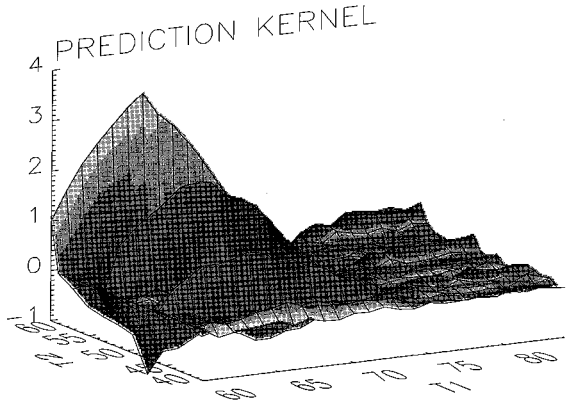

FIG. 1. The optimal prediction kernel $\Gamma_{opt}(t, t')$ of the NINO3 time series. Here, (T1, T2) represents (t, t') where t is time in prediction domain ($\mathcal{R}$ = [0, 84]) and t' is time in data domain ($\mathcal{D}$ = [0, 60]). Only the region $(t, t') \in [60, 84] \times [40, 60]$ is plotted.

where $\{Y_i(t)\}$ is a predictand vector field, $\{X_i(t)\}$ is a predictor vector field, $\mathbf{R}$ is a regression coefficient matrix, and $\{e_i(t)\}$ is a random error vector. Each component of predictand and predictor vector fields is a PC time series. The goal of a regression analysis is to minimize the regression error $\{e_i(t)\}$. Of course, prediction proceeds according to (13) without the regression error term.

In the CCA, MCA, and PCR analysis, the predictor field may, in general, be different from the predictand field. In this study, however, the predictor field is purposely set to be the same as the predictand field so that direct intercomparisons of different predictors are possible. The purpose is to examine the conceptual difference from the others and to demonstrate the utility of the present predictor. The three predictors above basically find a transformation between the predictor and the predictand fields, which results in the maximum correlation between the two fields. This transformation with maximum correlation allows the predictand field to be estimated reasonably in terms of the predictor field. The present method, on the other hand, uses temporal oscillation patterns for predicting future values. This is a significant difference between the present predictor and the other methods. Comparisons will reveal that the idea of extending temporal oscillation patterns in terms of temporal EOFs works fine and that the performance of the present predictor is comparable, if not superior, to those based on maximum correlations between the predictand and predictor fields.

Section 2 of this article includes one-dimensional prediction examples. A particular emphasis is given to El Niño–Southern Oscillation (ENSO) predictions. In this section, the present method is compared with the AR predictor since both are based on the minimization of the prediction error variance. Also comparisons with different prediction methods should be possible since there have been extensive studies accumulated over the

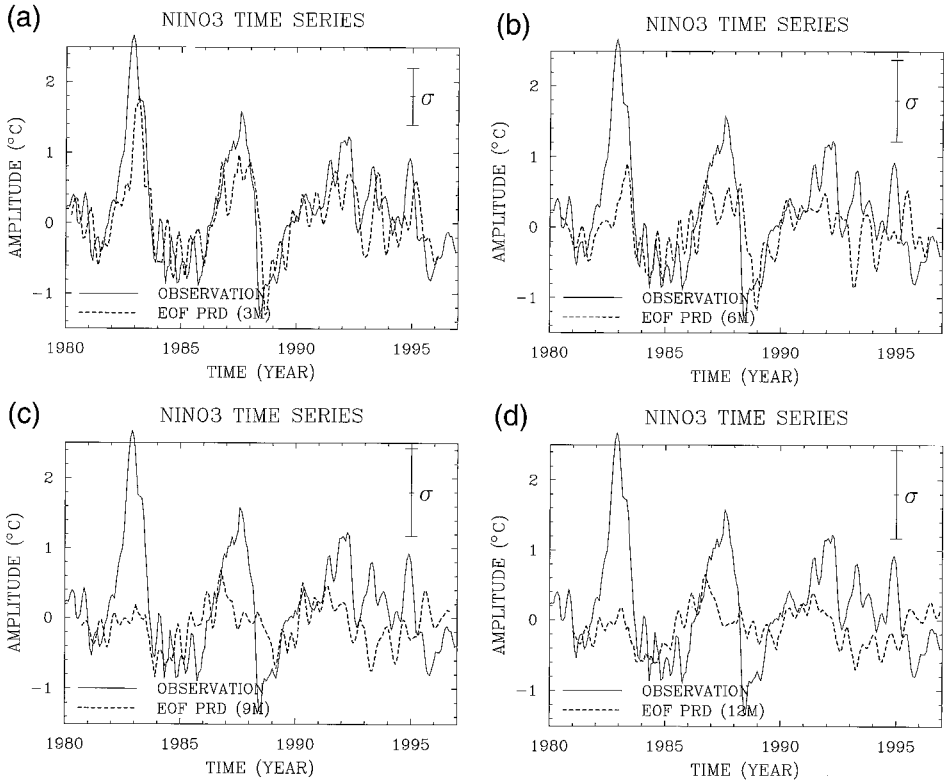

FIG. 2. Plot of smoothed monthly NIÑO3 time series (solid line) and predictions (dotted lines) at various lead times with one standard deviation of prediction errors. The NIÑO3 time series was smoothed via running mean with the lag of 3 points (±1 month) before being used for prediction.

past decade or so. Section 3 discusses a two-dimensional prediction example. It concerns the prediction of spatial patterns of El Niños. In this section, the performance of the present predictor is compared with four different statistical predictors frequently used in practice in the El Niño predictions. Some concluding remarks follow in section 4.

2. One-dimensional applications

Included here are one-dimensional (1D) applications of the EOF-based predictor developed in Kim and North (1998). The first dataset represents a 47-yr (1950–96) time series of the monthly SST in the NIÑO3 area (5°N–5°S and 150°–90°W). The El Niño condition is identified with warmer SST on the eastern side of the Pacific and the La Niña condition with colder SST than normal.

Prior to prediction the observational data was smoothed via three-point running averaging, which utilizes data 1 month in the future. (Alternatively, one can construct a smoothed 1D time series from a two-dimensional field that is smoothed via EOF truncation.) This smoothing increases the correlation scale rather significantly. It is necessary in a statistical prediction that high-frequency fluctuations, both in space and time, be removed for improved predictability.

It should be noted that actual lead time is 1 month shorter than nominal lead time in predicting smoothed time series since three-point smoother uses one point in the future. Of course, estimating actual (monthly) observations from moving averages requires one additional future point. As a result, prediction skill for the raw (monthly) data will be reduced by 2 months. There is an argument, however, that short-scale fluctuations (of Nyquist frequency) are not part of El Niño and may represent background noise and removing them benefits the prediction of El Niño. Namely, smoothed data may be a better representation of El Niño, which could be a biased opinion of the authors. At any rate, the prediction of a 3-month moving-averaged SST field is fairly common in practice (see, e.g., the climate diagnostics bulletin published by the U.S. Department of Commerce). In the following, nominal lead time is used and the results should be understood as described above.

The covariance function of the time series (not shown) was computed based on the first 32 yr of data and is similar to that of a second-order Markov process with some oscillatory behavior (Kim and North 1998). It decays rapidly to zero with increasing lag with a correlation length scale of about 6.5 months. This indicates an inherent limit in the statistical predictability of ENSO. The optimal prediction kernel of the NINO3

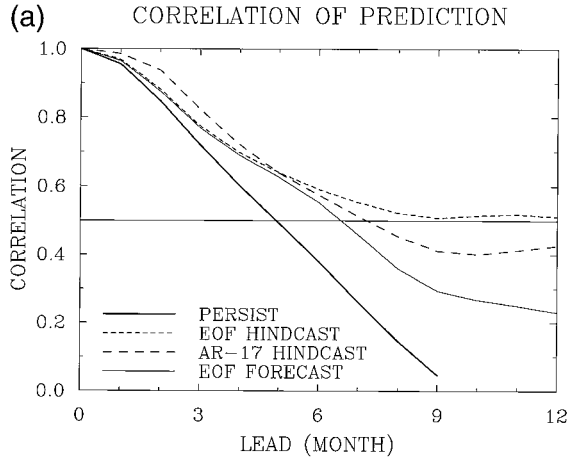

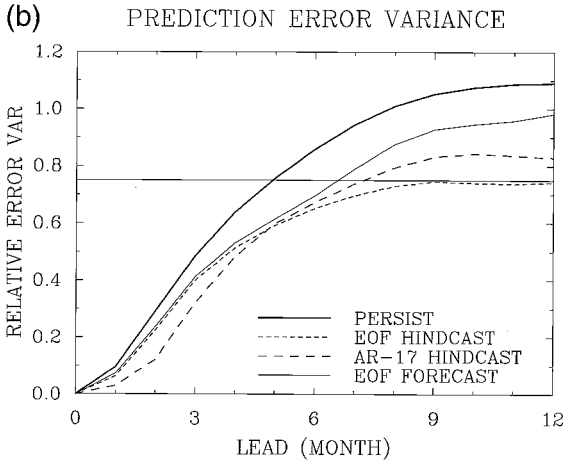

FIG. 3. (a) Plot of correlation and (b) prediction error variance of the persistence (thick solid line), hindcasting of the EOF predictor (dotted line), hindcasting of the AR-17 predictor (dashed line), and forecasting of the EOF predictor (thin solid line). Significant prediction skill extends to about 6 months.

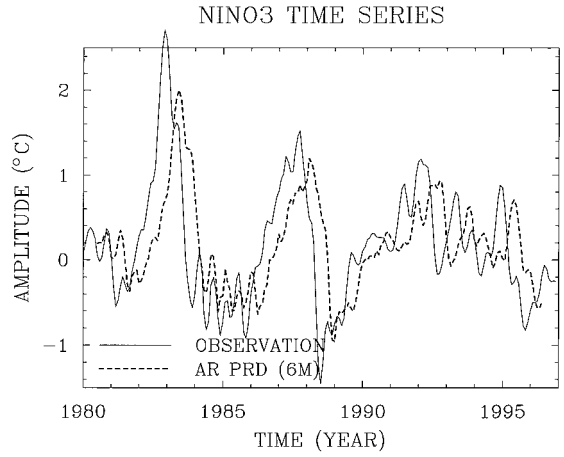

FIG. 4. Plot of smoothed monthly NIÑO3 time series (solid line) and AR-1 prediction (dotted lines) at 6-month lead time. A low-order AR model cannot predict semiperiodic components in the data satisfactorily.

time series is shown in Fig. 1. It is similar to that of the second-order Markov process (e.g., Fig. 6 in Kim and North 1998) but the shape is more irregular. Predictability decays rapidly away from the data domain boundary into the future with some undulations in the prediction kernel indicating the presence of some oscillatory processes.

Figure 2 shows predictions of the SST time series at four different lead times. Note that the prediction forward of 1982 is a ''forecast'' since the prediction filter is computed based only on the data prior to 1982. The data domain (length of the filter) is 60 months long, which barely covers the major periodicity of El Niño. The prediction filter is updated at every step with new observational data for forecasting. As shown in the figure, predicted values are fairly similar to the observed values up to the lead time of about 6 months. At the lead time of 6 months the onset of major El Niño occurrences was rather reasonably predicted although the exact timing was not captured. At the lead time of 9 months and longer, the predictor seriously underestimates the major peaks in the observational data. There is still some predictability as evidenced by concurrent peaks in the data and in the prediction. Since the predictor is purely statistical, this predictability should come from low-frequency fluctuations of the data (Barnett et al. 1988, 1994).

The correlation and the relative prediction error variance of the predictor for the SST time series are shown in Fig. 3. The Brier-based skill score is given in terms of relative prediction error variance σ_e^2/σ^2 (see Livezey 1995):

$$\beta = 1 - \frac{\sigma_e^2}{\sigma^2} = 2\rho\left(\frac{\sigma_f}{\sigma}\right) - \left(\frac{\sigma_f}{\sigma}\right)^2, \qquad (14)$$

where ρ is the correlation between forecast and raw data; and σ, σ_f, and σ_e are standard deviation of raw data, forecast, and prediction error, respectively. The minimum value of β is 0.25 for $\rho \geq 0.5$ and $(\sigma_f/\sigma) \geq 0.5$. Note that the latter requirement is enforced because statistical predictors tend to underestimate σ_f. Thus, the prediction skill here is defined as the maximum lead time for which correlation between observation and prediction is greater than 0.5 and relative prediction error variance is less than 0.75. NIÑO3 SST is reasonably predictable up to about 7 months in advance. The skill of the predictor is substantially better than the damped persistence at all lead times. The damped persistence is used hereafter, which is essentially an AR-1 prediction. Relative prediction error quickly approaches 100% (i.e., $\beta = 0$) as the lead time exceeds about 8 months. There is only a slight seasonal change in the predictability

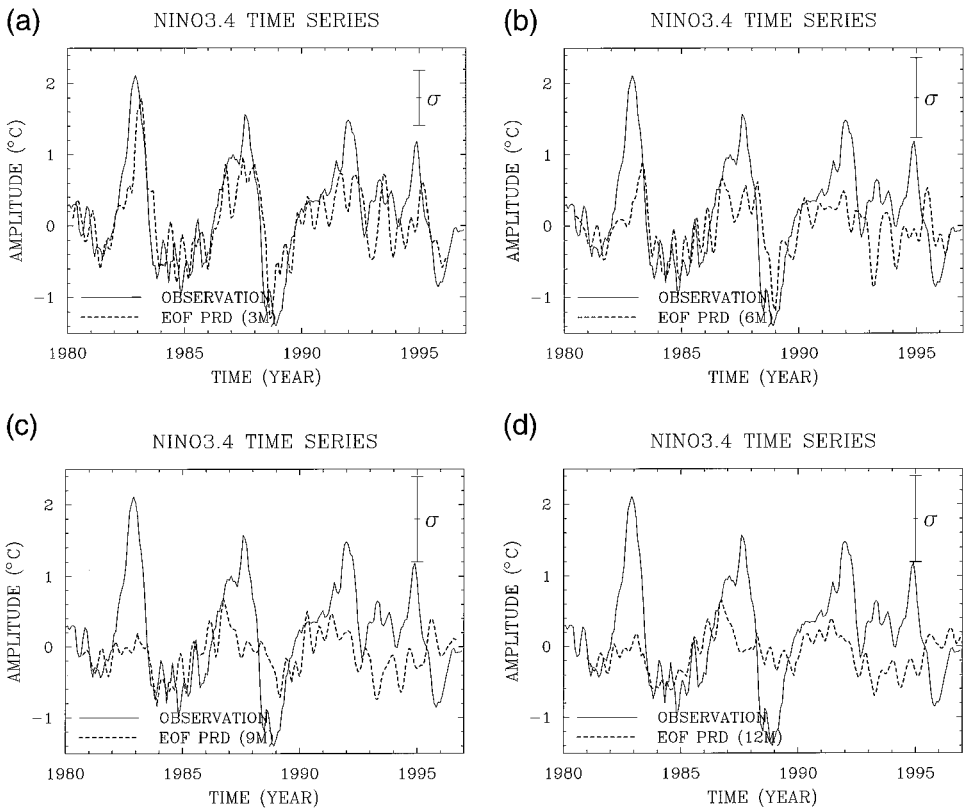

FIG. 5. Plot of smoothed monthly NIÑO3.4 SST time series (solid line) and predictions (dotted lines) at various lead times with one standard deviation of prediction errors. The SST time series was smoothed via running mean with the lag of 3 points (±1 month) before being used for prediction.

(figure not shown). There is no pronounced ''spring barrier'' in the predictability. In fact, the lowest predictability is in the winter. The result seems to be consistent with other seasonal ENSO prediction studies based on statistical approaches (Graham et al. 1987b; Barnett et al. 1988; Latif et al. 1994).

As shown in the figure the performance of the present predictor is almost the same as that of an order-17 AR predictor. This is a reasonable result since both methods are based on the minimization of prediction error. The computational difficulty and expense of the AR predictor is slightly less than the present predictor. The latter, however, is more flexible in terms of data smoothing via EOF truncation. Further, generalization of the AR method is not obvious for nonstationary processes such as cyclostationary processes. Note that the order of the best AR predictor is relatively high because of the presence of semiregular fluctuations in the dataset. They are identified as sharp, moderately high spectral peaks in the 2- to 6-yr band. It is often seen that the performance of a statistical predictor is compared with that of an order-1 AR predictor. A low-order AR model is typically ackward to model semiregular fluctuations. As shown in Fig. 4 prediction is a simple phase shift of the observational data with peaks slightly damped according to the damping scale of the AR model.

Finally, it should be emphasized that hindcasting and forecasting skills for the present predictor are not much different. This can be argued by reasoning that the covariance function should be almost the same when a small section of the record is discarded (resampling). In reality, however, covariance statistics are not truly stationary. They change from one time to another also partly due to sampling error. A small difference in the predictability reflects the combined effect of sampling error and slight nonstationarity.

The second dataset is the 47-yr (1950–96) time series of the SST in the NIÑO3.4 area (5°N–5°S and 170°–120°W). As in the previous example the observational data were smoothed via a 3-month running averaging. Then, the covariance function and the prediction filter were constructed based on the first 32 yr of the dataset. The length of the prediction filter is 60 months and it looks very similar to that in Fig. 1 for the NIÑO3 time series.

Figure 5 shows predictions of the SST time series at four different lead times. These predictions are hindcasting prior to 1982 and forecasting since 1982. As

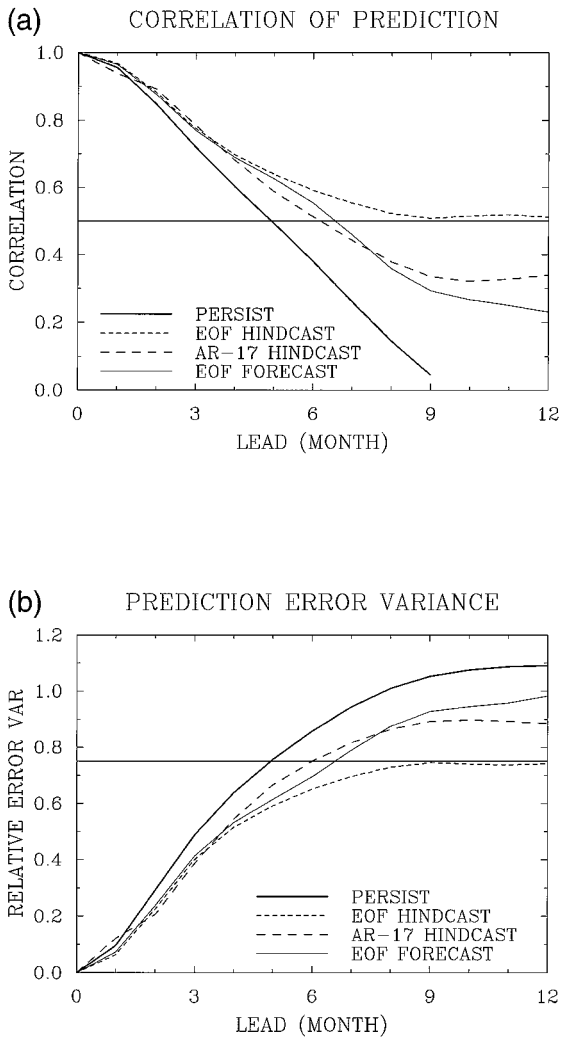

FIG. 6. (a) Plot of correlation and (b) prediction error variance of the persistence (thick solid line), the EOF predictor (dotted line), and the AR-17 predictor (dashed line). Significant prediction skill extends to about 6 months.

shown in the figure, the observed values were faithfully predicted up to the lead time of 6 months. The prediction of the amplitude and the onset of each El Niño is reasonable. In particular, the 1987–88 event was successfully predicted. At the lead times of 9 months and longer the predictor underestimates the observed El Niño and La Niña conditions. The 1982–83 event was poorly resolved.

The correlation and the relative prediction error variance of the predictor for the SST time series are shown in Fig. 6. Note that the prediction skill is not much different for hindcasting and forecasting for the present predictor. As in the earlier example, ENSO is reasonably predictable up to about 6 months in advance. The skill of the predictor is better than the persistence at all lead times. There is a slight seasonal variation in the predictability of El Niño. This seasonal variation in the predictability is rather different from other studies. There is no hint of the so-called spring barrier in the predictability. The performance of the present predictor is again almost the same as that of an AR predictor. The order of the best AR predictor (order 17) is fairly high in order to explain the semiregular fluctuations in the dataset. They are identified as moderately high spectral peak(s) in the ENSO band.

3. Two-dimensional applications

a. El Niño prediction comparisons

It is also useful to forecast the spatial patterns of El Niño. As delineated in Kim and North (1998) a two-dimensional (2D) prediction requires space–time EOFs of the prediction field. Major spatial patterns of the 40 yr (1950–89) of the tropical Pacific SST field are depicted in Fig. 7. The data covers the area (120°E–80°W) $\times$ (30°N–30°S) and is derived from the Comprehensive Ocean–Atmosphere Data Set (Woodruff et al. 1987). The dataset was smoothed via a 3-month running averaging prior to the computation of EOFs. These EOFs together explain about 60% of the total variability. The first two patterns have been identified to be similar to EOFs (e.g., Cane 1992; Chang et al. 1995; Wang et al. 1995) and POPs (Chang et al. 1996; Penland and Magorian 1993) of simulated SST anomalies (see also Fig. 11). In the experiment, the spatial extent of the data domain is the same as the prediction domain (Kim and North 1998). They differ only in the temporal extent.

Let us first examine the performance of five different statistical predictors. They are the POP, MCA, CCA, PCR, and EOF-based predictors. Note that the performance of CCA predictor is almost the same as MCA predictor and hence only MCA results are shown in the following. As mentioned earlier, prediction is conducted in the EOF space and the first 10 EOF modes have been retained. The predictors used here are in their most basic forms although some refined versions may currently be used in practice. In this experiment the predictor and predictand fields are the same although MCA and PCR can be used with a predictor field that is different from a predictand field. The predictor field is purposely set to be the same as the predictand field so that this exercise clearly depicts and compares the performance of the predictor based on temporal EOFs (present predictor) and the others based on the maximum correlations (MCA, CCA, PCR). In all the cases, the predictor is constructed based on the first 30 yr of data.

Figure 8 shows the NIÑO3 time series derived from the predicted 2D SST fields in comparison with the observation. At the 3-month lead time all the predictors reproduce reasonably the NIÑO3 SST time series although time lagging is rather obvious in all the predictions. At the 6-month lead time, lagging is more pronounced especially in the predictions based on the MCA

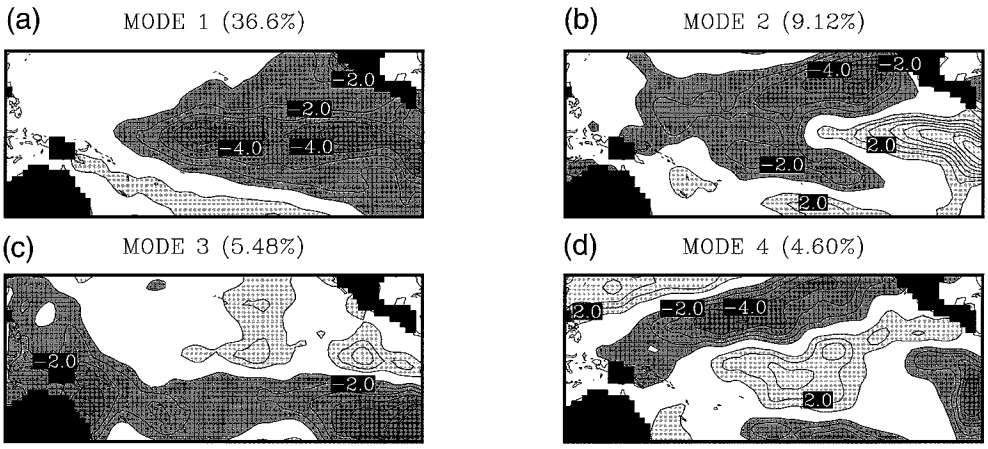

Fig. 7. Four dominant EOFs (with percent variance in parentheses) of the monthly surface temperature anomaly field. EOFs are computed based on the first 40 yr (1950–89) of data.

predictors. The performance of the predictors are summarized in Fig. 9. The EOF, POP, and PCR predictors do a moderate job with the prediction skill extending up to about 7 months. The performance of the MCA and the CCA predictors is not very satisfactory. In fact, the MCA and CCA predictors are only negligibly better than persistence at all meaningful lead times.

An example of maximum covariance patterns in the MCA analysis is shown in Fig. 10. The predictand field here is the same as the predictor field except that it is shifted backward in time by 12 months (i.e., 12-month lead time). The first CCA eigenvectors show that the first EOF pattern dominates the predictor field as should be expected and the second EOF pattern dominates the

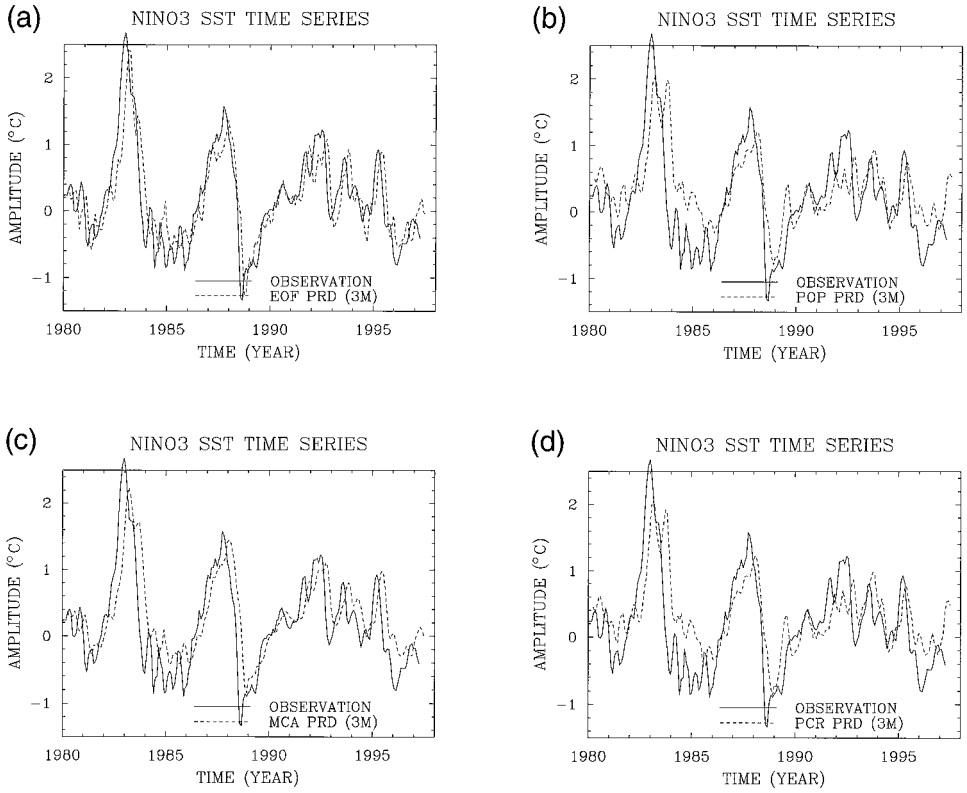

Fig. 8. Plot of smoothed NIÑO3 SST time series (solid line) and predicted time series (dotted lines) from two-dimensional predictions at 3- and 6-month lead times for four different predictors: (a),(e) EOF, (b),(f) POP, (c),(g) MCA,

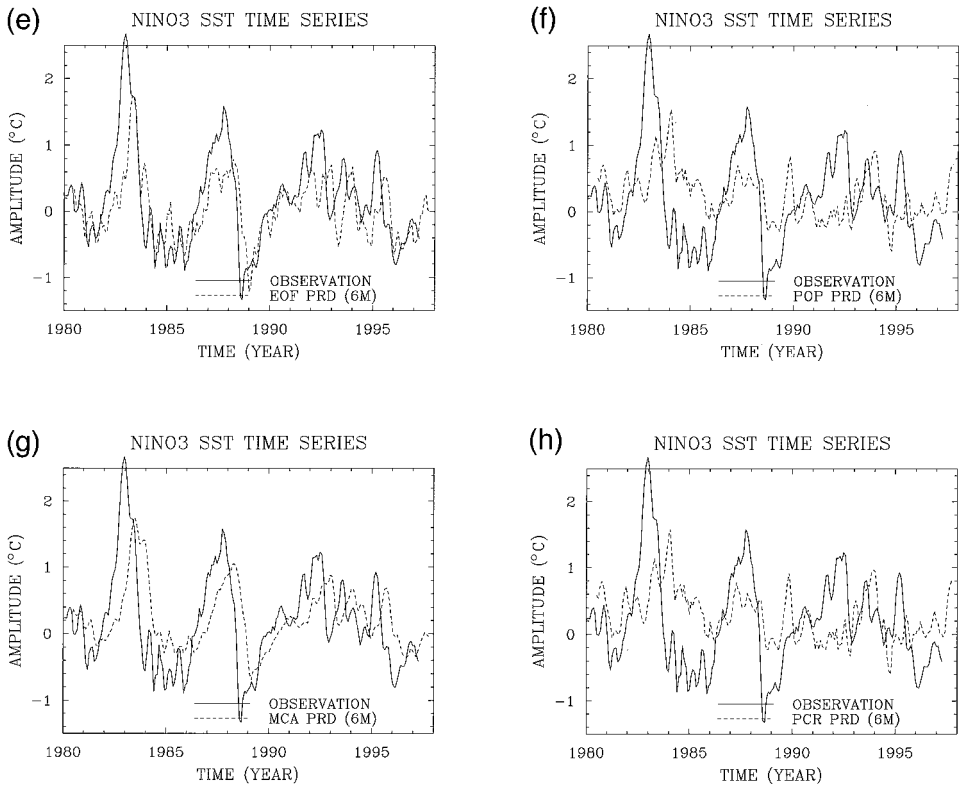

FIG. 8. (*Continued*) and (d),(h) PCR. The tropical Pacific SST dataset was smoothed via running mean with the lag of 3 months prior to the analysis.

predictand field. Bear in mind that the first two EOF modes are the typical patterns associated with El Niños (Fig. 7). In fact, they look similar to the third POP patterns with about a 27-month period (see Fig. 11). Thus, the first CCA patterns make sense. That is, if the first EOF mode is dominant in the predictor field then the second mode will be dominant in 12 months (or rather in half the period) because of their phase relationship. The second CCA pattern is more difficult to interpret. The third, fourth, and fifth EOF modes in the predictor field are correlated mainly with the first EOF mode at 12-month lead time. If the first and second EOF modes were exactly periodic one might expect that the second CCA patterns similar to the first CCA patterns with the dominance of the first and second EOF modes switched in the predictor and predictand fields. This seems to indicate the asymmetry of the El Niño phase progressions. Such pattern correlations do not explictly make use of the temporal evolution of patterns as was done in the developed predictor. The result is a surprisingly unsatisfactory prediction skill shown in Fig. 9.

The POP prediction is essentially based on the period and the decay time of POP modes, which are derived from the eigenvalues of POPs. Shown in Fig. 11 are the third POP mode and its adjoint pattern, which have great relevance to El Niño prediction (see also Penland and Magorian 1993). Indeed, the imaginary and real parts of the third POP clearly resemble the first and the second EOFs, respectively. The period of the mode is 27 months, which is in the period range (2 to 6 yr) of the observed El Niños. Figure 12 shows the AR spectra of the real and imaginary parts of the third POP PC time series, which were smoothed by using the singular spectral analysis (Dettinger et al. 1995; Vautard et al. 1992). The spectral peaks are at somewhat different periods than that derived from the eigenvalue (27 months). Actually there is only a little power at the given periodicity indicating a weak cyclicity of the identified patterns. The figure also indicates the sensitivity of the POP period. Thus, it is necessary to examine whether the oscillation of major POP patterns is regular or not prior to prediction exercise. This requirement seems to be reasonably satisfied by the sea level pressure dataset (Xu and von Storch 1990).

b. El Niño pattern predictions

Figure 13 shows the observed and predicted SST fields from September 1982 to January 1983 using the developed predictor. The prediction is at the lead time of 3 months. This exercise is forecasting since only past observational data have been used in constructing the

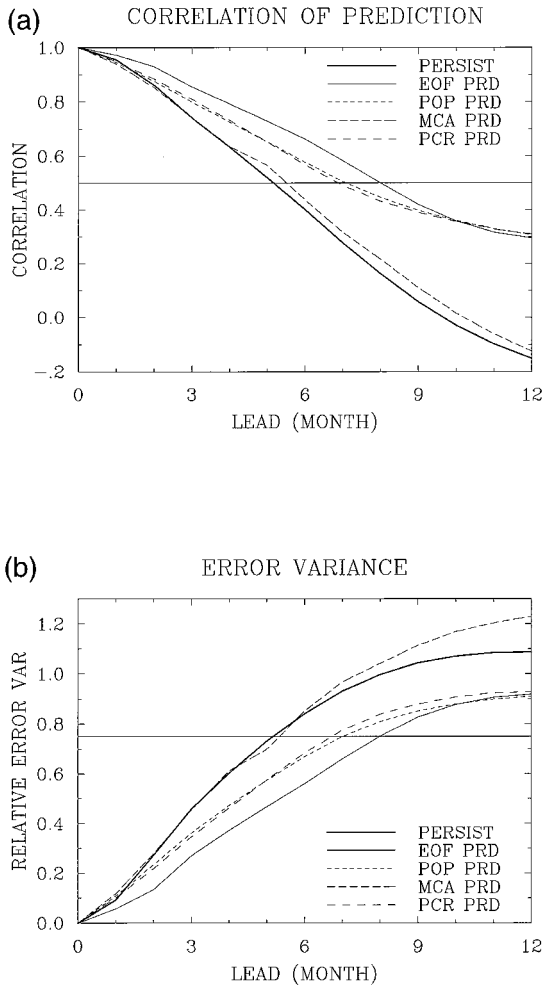

FIG. 9. (a) Plot of correlation and (b) prediction error variance of the persistence (thick solid), the EOF predictor (dotted), the POP predictor (short dashed), the MCA predictor (dashed), and the PCR predictor (long dashed). The result is based on the data in the interval 1955–96.

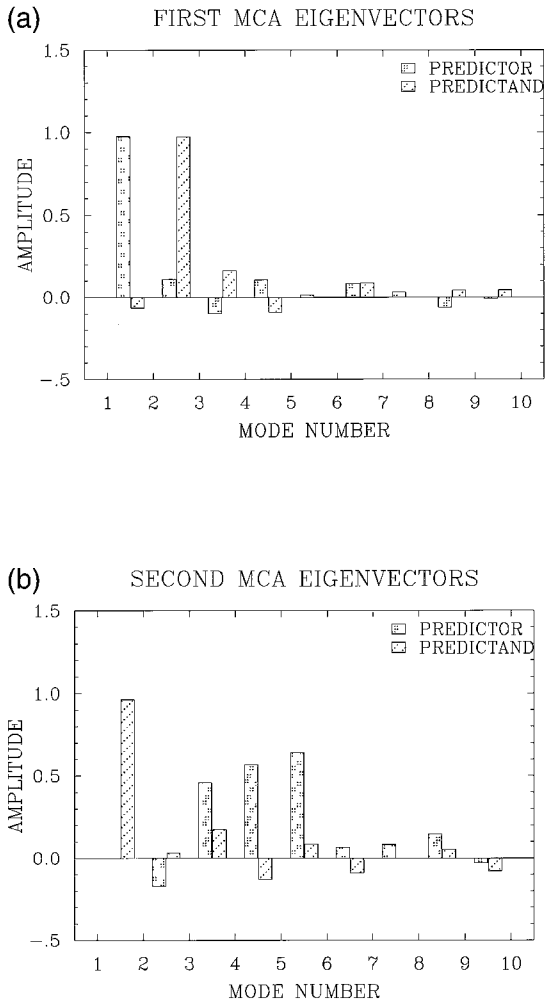

FIG. 10. The first two eigenfunctions of the MCA analysis. (a) The first dataset is the tropical Pacific SST field truncated in terms of 10 EOFs (predictor) and (b) the second dataset is the same field but is shifted backward in time by 12 months (predictand).

spatial covariance function, which then was used to compute the EOFs. Only 18 EOF modes have been used for prediction, which explain about 80% of the total variability. The neglected EOFs seem to represent background noise and may be irrelevant for El Niño prediction. In the comparisons the observational data were also smoothed in terms of 18 EOFs. As shown in the figure, the predicted fields are somewhat underestimated even at this short lead time. The predicted El Niño pattern, however, is fairly similar to that in the observational data. The onset of the 1982/83 El Niño was not accurately captured with the significant delay in the prediction. This delay is also obvious in Fig. 8. It should be noted that the underestimation and the retardation of the predicted field are common and inherent features for many different statistical and dynamical predictors (e.g., Barnett et al. 1993; Penland and Magorian 1993).

During the period of September 1987 to January 1988, forecasted SST fields similarly underestimated the observational data (Fig. 14). The prediction delay is not serious in this case and the spatial patterns of this fully developed stage of ENSO were faithfully reproduced at the lead time of 3 months. The observed and the predicted SST fields were also plotted in Fig. 15 for the period of October 1991 to February 1992. There is not much phase retardation in the predicted field. The predictions from November to December 1991 are unsatisfactory with the spatial patterns of the El Niño not well reproduced. In fact, most predictors have a varying degree of difficulty in forecasting this El Niño. These forecasts demonstrate the utility of the developed predictor. Although there is some apparent delay the predicted patterns, nevertheless, are reasonable. The pre-

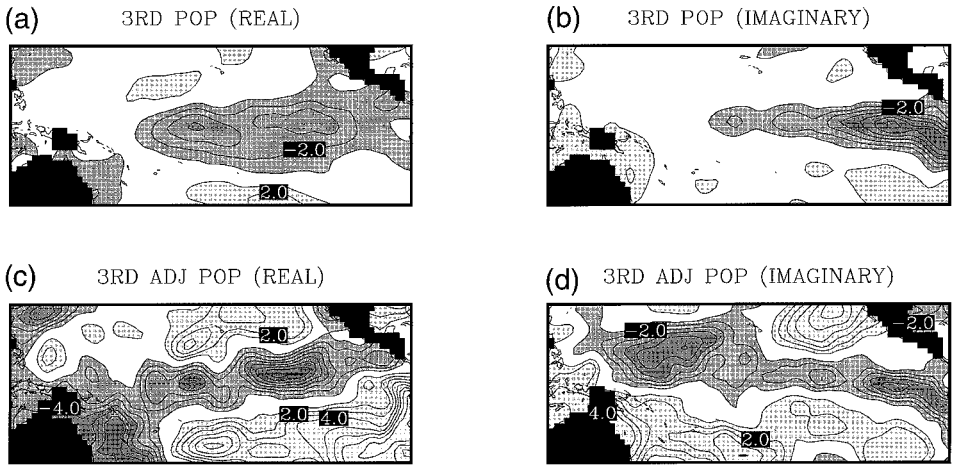

FIG. 11. The (a) real and (b) imaginary patterns of the third POP and (c,d) the corresponding adjoint POP derived from the first 30 yr of the tropical Pacific SST dataset. This particular POP has the period of 27 months and the dampling scale of 8.4 months.

diction seems to somewhat underestimate the observed field most of the time.

Finally, Fig. 16 shows the prediction skill of the two-dimensional predictor for the monthly SST anomaly field. Correlation between the observed and predicted fields was based on the 42 yr (1955–96) of data. Note again that both the observed and the predicted fields were smoothed in terms of 18 EOFs. We assume that the neglected EOFs represent ''noise'' patterns irrelevant with the prediction of El Niños. The spatial patterns of El Niño are predictable reasonably (correlation greater than 0.5) more than about 6 months in advance. The correlation skill of the predictor is better than persistence at all the lead times. Predictability increases to about 9 months along the tropical equatorial belt in the spring. There is not much seasonal variation in the predictability of El Niño. Also, significant skill is not confined in the narrow equatorial band as in other dynamical studies. This may be because EOFs and POPs from numerical models are much narrower in latitudinal extent than those of observational data.

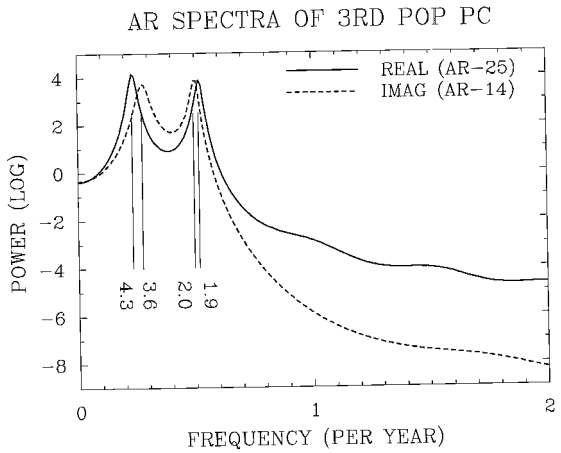

FIG. 12. The AR spectra of the real and imaginary parts of the third POP PC time series. The original PC time series have been smoothed in terms of singular spectral analysis with window length 72 months (6 yr) and four singular spectral modes have been retained.

4. Summary and concluding remarks

Considered here were the applications of the general statistical predictor developed in Kim and North (1998). The predictor is based on the minimization of the prediction error variance. All the examples demonstrate that the performance of the developed predictor is reasonable and that it is a useful tool for climate studies. The developed predictor is computationally simple and efficient and yet achieves the maximum linear predictability that a dataset affords under the stationarity assumption. Although dynamical methods should eventually outperform statistical methods as models are continually being improved (e.g., Behringer et al. 1998; Ji et al. 1998), the developed predictor seems to be a simple and useful tool for routine prediction exercises including El Niño predictions.

The performance of the AR predictor is similar to that of the present predictor since both methods are based on the minimization of prediction error variance. In the former method an optimal order of the AR model should first be found for prediction. The optimal orders are generally high in El Niño applications. The performance of a low-order AR predictor is poor with the sign of significant phase delay. On the other hand, the developed predictor requires accurate EOFs, which in turn require a sufficiently long dataset. For a short record (less than three times the length of prediction domain), the performance of the EOF-based predictor will be sub-

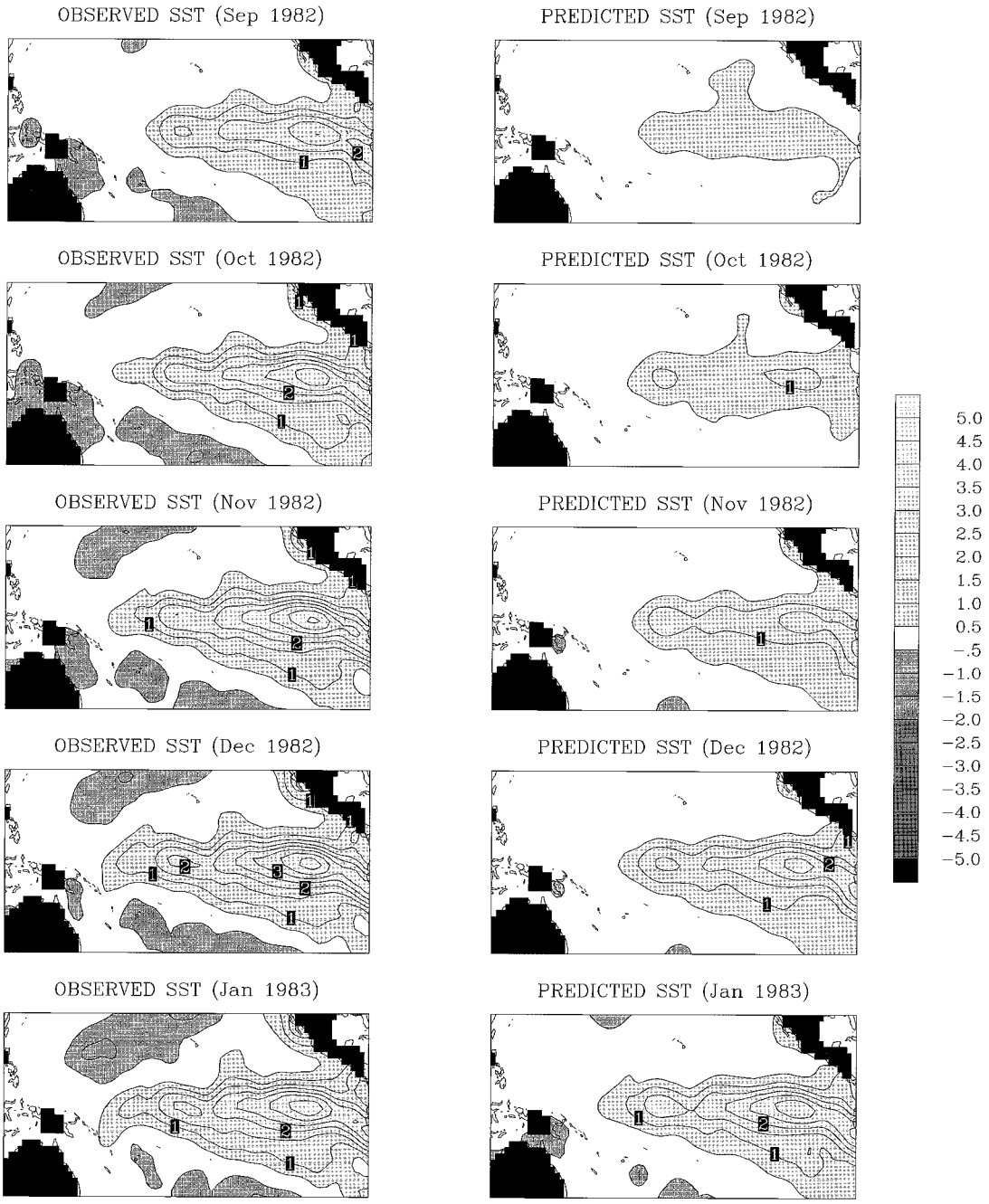

FIG. 13. Observed and forecasted SST fields from Sep 1982 to Jan 1983 at lead time of 3 months. The observed fields were smoothed in terms of 18 EOFs, which explain 80% of the total variability.

optimal and a high-order AR model may be a better choice.

The present predictor is conceptually different from other predictors that utilize correlation patterns between the predictor and predictand fields as a means of prediction. The developed predictor makes use of the temporal patterns of fluctuation derived from past observations of a predictand field. This was done in terms of space–time EOFs. A comparison shows that the idea works well. According to the limited test, the performance of the EOF-based predictor is slightly better than those based on maximum pattern correlations or POPs. The POP predictor finds major spatial patterns and the associated periodicities and damping scales of a predictand field. Often, the period and damping scale of a POP pattern are not accurate since a multivariate AR-

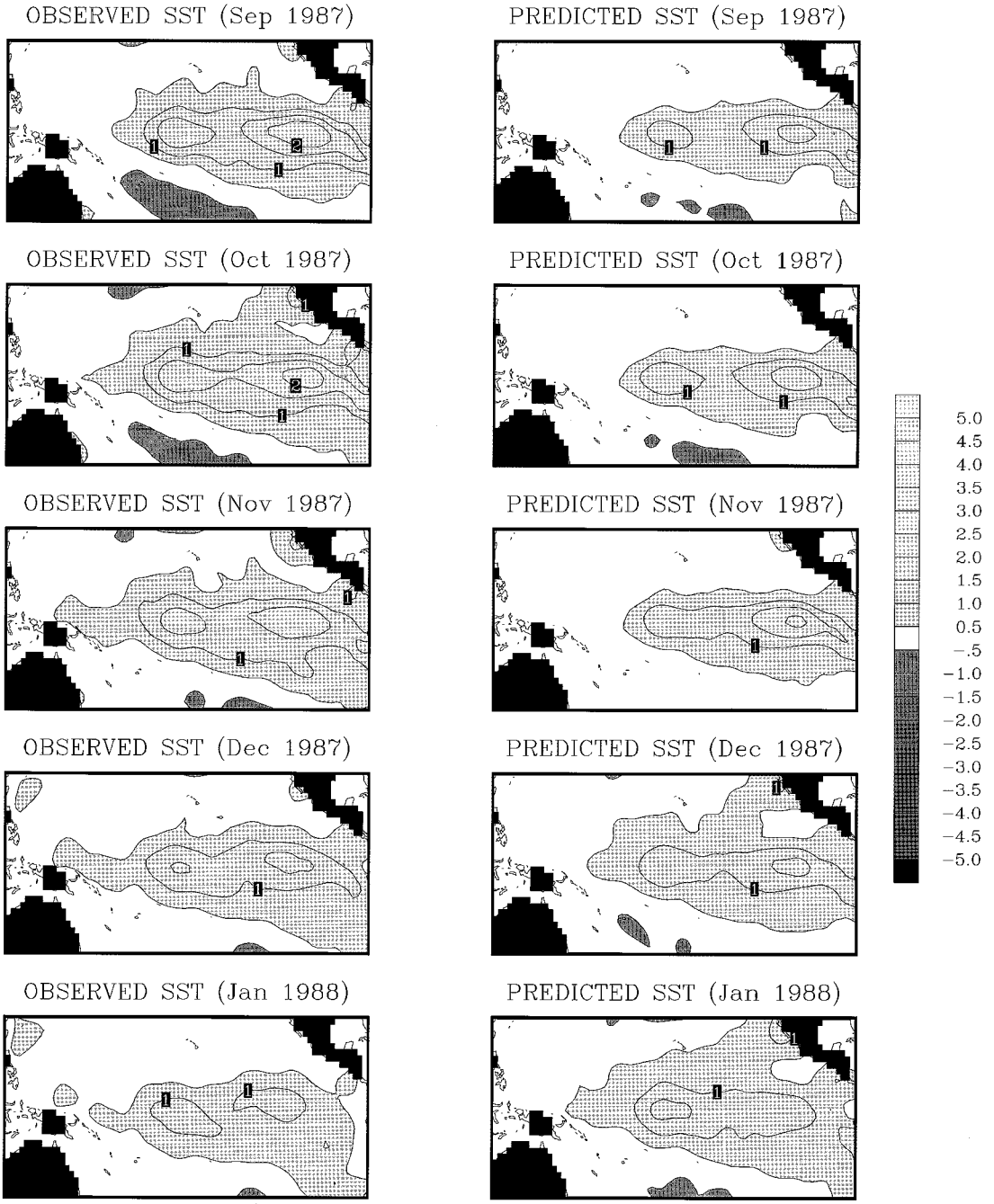

FIG. 14. Same as Fig. 13 but for the period of Sep 1987 to Jan 1988.

1 model like POP is incapable of accurately extracting complex and multiple periodicities. Further, it is difficult to argue that the El Niño patterns have regular periodicities.

Some interesting results from 1D El Niño prediction examples are the following. 1) The El Niños were forecasted reasonably up to about 6 months from the NINO3 and NINO3.4 time series, which were smoothed in terms of a 3-month moving averaging (e.g., Latif et al. 1994). High-frequency fluctuations in the dataset have been removed prior to prediction exercise on the ground that they may represent background noise. The performance of the predictor much degrades in the presence of high-frequency fluctuations. The resulting prediction skill, with the consideration of 3-month smoothing, is much better than the persistence and seems to be in the general

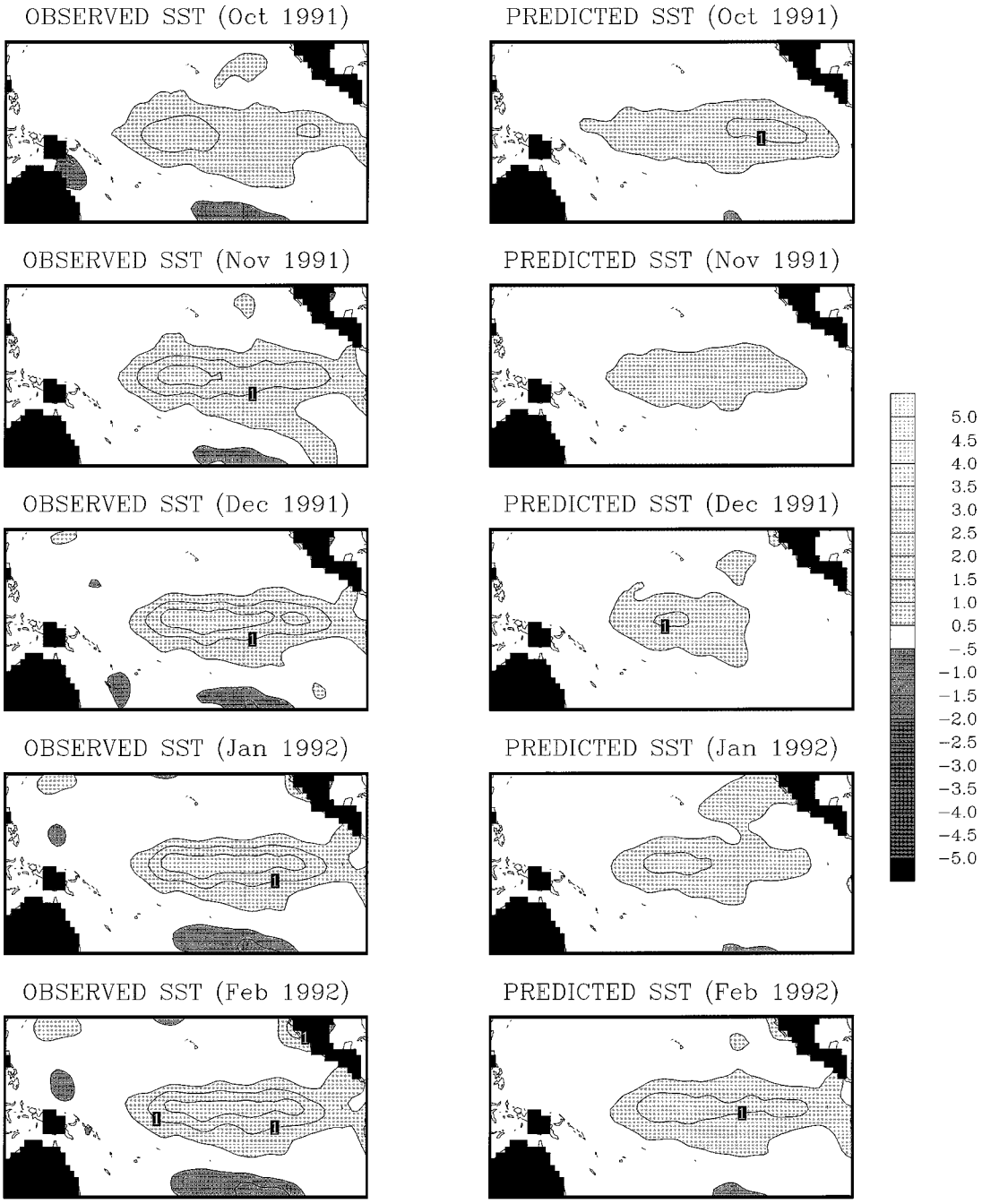

FIG. 15. Same as Fig. 13 but for the period of Oct 1991 to Feb 1992.

range of predictability of other elaborate predictors including Barnett et al. (1988), Xu and von Storch (1990), and Penland and Magorian (1993). The prediction skill is lower than that of some dynamical approaches using models (e.g., Cane et al. 1986; Latif and Flügel 1991; Latif et al. 1994; Chen et al. 1995; Ji et al. 1996, 1998). 2) The main source of predictability in the present approach are low-frequency fluctuations in the data. Such low-frequency fluctuations are reasonably well reproduced and extended (in time) in terms of temporal EOFs. Judging from the reasonable prediction skill of the present technique over a fair extend of lead time, such low-frequency fluctuations indeed characterize ENSO events approximately. 3) As in many other studies, the predictability of El Niño is seasonally dependent. The spring barrier, however, is not so apparent as in other

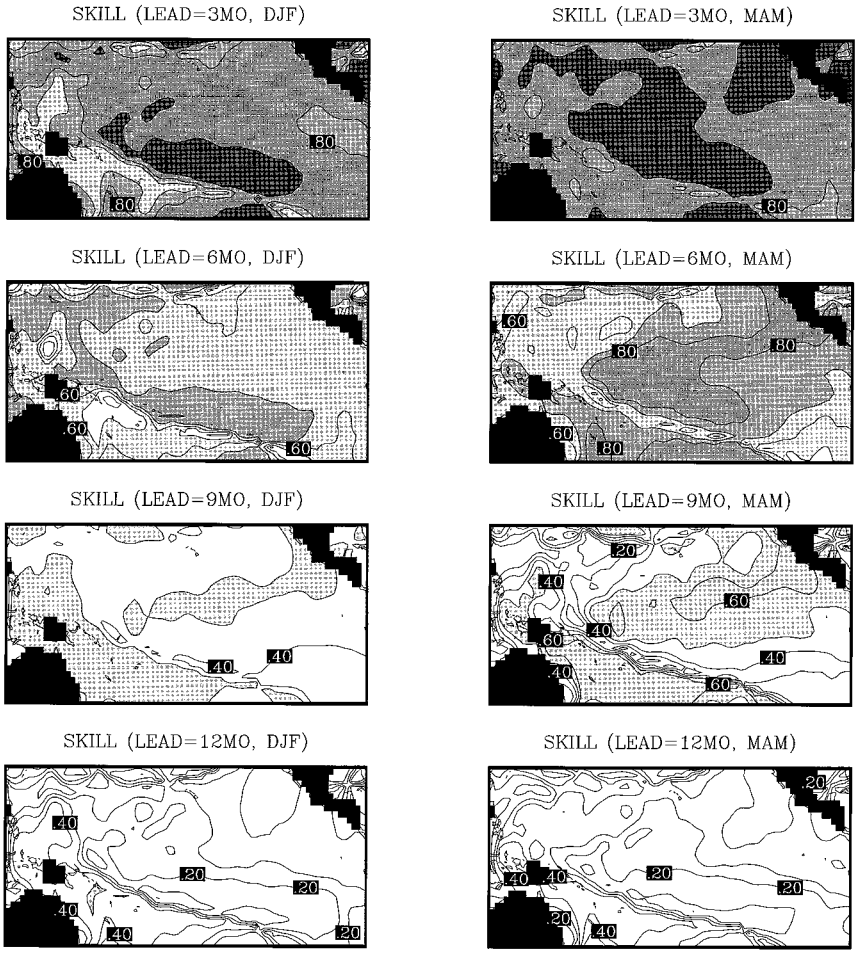

FIG. 16. Prediction skill of the 2D linear predictor for the monthly SST field. The SST field was smoothed via a 3-month running averaging. The prediction skill here is based on the reconstructions taking only 18 EOFs, which explain about 90% of the total variability.

studies. The seasonal dependency seems to be associated with the seasonal phase locking of the SST anomalies (Balmaseda et al. 1995) and the seaonal variation in the basic state or background statistics (Chen et al. 1995; Davey et al. 1996). A plausible explanation for the lack of spring barrier seems to lie in the decadal variations of the proposed mechanisms.

Results from 2D examples are as follows. 1) The spatial patterns of El Niño after a 3-month moving averaging were predicted reasonably up to 6 months ahead over the entire equatorial Pacific basin. The predictability has strong geographic dependency with somewhat larger predictability in the eastern and central Pacific. Along the tropical equatorial belt El Niño can be predicted up to about 9 months. There is also a weak seasonal dependency with stronger predictability in the spring. 2) In 2D examples, phase delay in the prediction is an obvious problem for all the statistical predictors considered in this study. The phase delay occasionally is as large as the lead time making the prediction useless. Also, underestimation of the predictand field is another obvious problem. All the statistical predictors underestimate the predictand field in general.

There is also a further improvement to be made. In some prediction studies, it may be beneficial to include the phase information. For one thing, statistics of the data may not be stationary. Statistics of the surface temperature field, for example, exhibit significant seasonal dependency (Kim et al. 1996; Kim and North 1997). Also some phenomena such as El Niño may be strongly phase locked with the seasonal cycle (Jin et al. 1994; Tziperman et al. 1994; Chang et al. 1994, 1995). This phase dependency of the predictor can be incorporated easily by using CSEOFs (Kim et al. 1996; Kim and North 1997). The predictor developed in Kim and North (1998) can easily be generalized for any complete basis set.

Acknowledgments. We thank anonymous reviewers for the critical reviews of the paper. Their comments

have been essential in making the final version of this paper. We express our gratitude to Dr. Penland (CIRES) for generously making her POP prediction programs available to us and also useful comments and discussion. We also thank Drs. Flügel and Chang at Texas A&M University for many useful comments. We gratefully acknowledges support for this work by the Dept. of Energy (DE-FG03-98ER62610) via a grant to Texas A&M University. The Department of Energy does not necessarily endorse any of the conclusions drawn in the paper.

REFERENCES

Balmaseda, M. A., M. K. Davey, and D. L. T. Anderson, 1995: Decadal and seasonal dependence of ENSO prediction skill. *J. Climate,* **8,** 2705–2715.

Barnett, T., N. Graham, M. A. Cane, S. E. Zebiak, S. Dolan, J. J. O'Brien, and D. Legler, 1988: On the prediction of the El Niño of 1986–1987. *Science,* **241,** 192–196.

——, M. Latif, N. Graham, M. Flügel, S. Pazan, and W. White, 1993: ENSO and ENSO-related predictability. Part I: Prediction of equatorial Pacific sea surface temperature with a hybrid coupled ocean–atmosphere model. *J. Climate,* **6,** 1545–1566.

——, and Coauthors, 1994: Forecasting global ENSO-related climate anomalies. *Tellus,* **46A,** 381–397.

Battisti, D. S., and A. C. Hirst, 1989: Interannual variability in a tropical atmosphere–ocean model: Influence of the basic state, ocean geometry, and nonlinearity. *J. Atmos. Sci.,* **46,** 1687–1712.

Behringer, D. W., M. Ji, and A. Leetmaa, 1998: An improved coupled model for ENSO prediction and implications for ocean initialization. Part I: The ocean data assimilation system. *Mon. Wea. Rev.,* **126,** 1013–1021.

Bretherton, C. S., C. Smith, and J. M. Wallace, 1992: An intercomparison of methods for finding coupled patterns in climate data. *J. Climate,* **5,** 541–560.

Cane, M. A., 1992: Tropical Pacific ENSO models: ENSO as a mode of the coupled system. *Climate System Modeling,* K. E. Trenberth, Ed., Cambridge University Press, 583–614.

——, S. E. Zebiak, and S. C. Dolan, 1986: Experimental forecasts of El Niño. *Nature,* **321,** 827–832.

——, M. Münnich, and S. E. Zebiak, 1990: A study of self-excited oscillations of the tropical ocean–atmosphere system. Part I: Linear analysis. *J. Atmos. Sci.,* **47,** 1562–1577.

Chang, P., B. Wang, T. Li, and L. Ji, 1994: Interactions between the seasonal cycle and the southern oscillation—Frequency entrainment and chaos in a coupled ocean–atmosphere model. *Geophys. Res. Lett.,* **21,** 2817–2820.

——, L. Ji, B. Wang, and T. Li, 1995: Interactions between the seasonal cycle and El Niño–Southern Oscillation in an intermediate coupled ocean–atmosphere model. *J. Atmos. Sci.,* **52,** 2353–2372.

——, ——, H. Li, and M. Flügel, 1996: Chaotic dynamics versus stochastic processes in El Niño–Southern Oscillation in coupled ocean–atmosphere models. *Physica D,* **98,** 301–320.

Chen, D., S. E. Zebiak, A. J. Busalacchi, and M. A. Cane, 1995: An improved procedure for El Niño forecasting: Implications for predictability. *Science,* **269,** 1699–1702.

Davey, M. K., D. L. T. Anderson, and S. Lawrence, 1996: A simulation of variability of ENSO forecast skill. *J. Climate,* **9,** 240–246.

Dettinger, M. D., M. Ghil, C. M. Strong, W. Weibel, and P. Yiou, 1995: Software expedites singular-spectral analysis of noisy time series, *Eos, Trans. Amer. Geophys. Union,* **76,** 12–21.

Draper, N. R., and H. Smith, 1981: *Applied Regression Analysis.* 2d ed. John Wiley and Sons, 709 pp.

Glahn, H. R., 1968: Canonical correlation and its relationship to discriminant analysis and multiple regression. *J. Atmos. Sci.,* **25,** 23–31.

Graham, N. E., and W. B. White, 1988: The El Niño cycle: A natural oscillator of the Pacific ocean–atmosphere system. *Science,* **24,** 1293–1302.

——, J. Bichaelsen, and T. P. Barnett, 1987a: An investigation of the El Niño–Southern Oscillation cycle with statistical models. 1. Predictor field characteristics. *J. Geophys. Res.,* **92,** 14 251–14 270.

——, ——, and ——, 1987b: An investigation of the El Niño–Southern Oscillation cycle with statistical models. 2. Model results. *J. Geophys. Res.,* **92,** 14 271–14 289.

Hasselmann, K., 1988: PIPs and POPs—A general formalism for the reduction of dynamical systems in terms of principal interaction patterns and principal oscillation patterns. *J. Geophys. Res.,* **93,** 11 015–11 020.

Ji, M., A. Leetmaa, and V. E. Kousky, 1996: Coupled model predictions of ENSO during the 1980s and the 1990s at the National Center for Environmental Prediction. *J. Climate,* **9,** 3105–3120.

——, W. Behringer, and A. Leetmaa, 1998: An improved coupled model for ENSO prediction and implications for ocean initialization. Part II: The coupled model. *Mon. Wea. Rev.,* **126,** 1022–1034.

Jin, F.-F., J. D. Neelin, and M. Ghil, 1994: El Niño on the devil's staircase: Annual subharmonic steps to chaos. *Science,* **264,** 70–72.

Kim, K.-Y., and G. R. North, 1997: EOFs of harmonizable cyclostationary processes. *J. Atmos. Sci.,* **54,** 2416–2427.

——, and ——, 1998: On EOF-based linear prediction algorithm: Theory. *J. Climate,* **11,** 3046–3056.

——, ——, and J. Huang, 1996: EOFs of one-dimensional cyclostationary time series: Computations, examples, and stochastic modeling. *J. Atmos. Sci.,* **53,** 1007–1017.

Latif, M., and M. Flügel, 1991: An investigation of short range climate predictability in the tropical Pacific. *J. Geophys. Res.,* **96,** 2661–2673.

——, T. P. Barnett, M. A. Cane, M. Flügel, N. E. Graham, H. von Storch, J.-S. Xu, and S. E. Zebiak, 1994: A review of ENSO prediction studies. *Climate Dyn.,* **9,** 167–179.

Livezey, R. E., 1995: The evaluation of forecasts. *Analysis of Climate Variability,* H. von Storch and A. Navarra, Eds., Springer, 177–196.

Münnich, M., M. A. Cane, and S. E. Zebiak, 1991: A study of self-excited oscillations of the tropical ocean–atmosphere system. Part II: Nonlinear cases. *J. Atmos. Sci.,* **48,** 1238–1248.

Newton, H. J., 1988: *TIMESLAB: A Time Series Analysis Laboratory.* Wadsworth and Brooks, 623 pp.

Penland, C., 1989: Random forcing and forecasting using principal oscillation pattern analysis. *Mon. Wea. Rev.,* **117,** 2165–2185.

——, and T. Magorian, 1993: Prediction of Niño 3 sea surface temperatures using linear inverse modeling. *J. Climate,* **6,** 1067–1076.

Suarez, M. J., and P. S. Schopf, 1988: A delayed action oscillator for ENSO. *J. Atmos. Sci.,* **45,** 3283–3287.

Tziperman, E., L. Stone, M. A. Cane, and H. Jarosh, 1994: El Niño chaos: Overlapping of resonances between the seasonal cycle and the Pacific ocean–atmosphere oscillator. *Science,* **264,** 72–74.

Vautard, R., P. Yiou, and M. Ghil, 1992: Singular-spectral analysis: A toolkit for short, noisy, chaotic signals. *Physica D,* **58,** 95–126.

von Storch, H., 1995: Spatial patterns: EOFs and CCA. *Analysis of Climate Variability,* H. von Storch and A. Navarra, Eds., Springer, 227–258.

——, and F. Zwiers, 1998: *Statistical Analysis in Climate Research.* Cambridge University Press, in press.

——, G. Bürger, R. Schnur, and J.-S. von Storch, 1995: Principal oscillation patterns: A review. *J. Climate,* **8,** 377–400.

von Storch, J.-S., 1995: Multivariate statistical modeling: POP-model as a first-order approximation. *Analysis of Climate Variability,* H. von Storch and A. Navarra, Eds., Springer, 281–298.

Wallace, J. M., C. Smith, and C. S. Bretherton, 1992: Singular value decomposition of sea surface temperature and 500-mb height anomalies. *J. Climate,* **5,** 561–576.

Wang, B., T. Li, and P. Chang, 1995: An intermediate model of the tropical Pacific Ocean. *J. Phys. Oceanogr.,* **25,** 1599–1616.

Woodruff, S. D., R. J. Sultz, R. L. Jenne, and P. M Steurer, 1987: A Comprehensive Ocean–Atmosphere Data Set. *Bull. Amer. Meteor. Soc.,* **68,** 1239–1250.

Xu, J.-S, and H. von Storch, 1990: Predicting the state of the Southern Oscillation using principal oscillation pattern analysis. *J. Climate*, **3,** 1316–1329.

Yu, Z.-P., P.-S. Chu, and T. Schroeder, 1997: Predictive skills of seasonal to annual rainfall variations in the U.S. Affiliated Pacific Islands: Canonical correlation analysis and multivariate principal component regression approaches. *J. Climate*, **10,** 2586–2599.